Indian J Phys. **71B** (5), 545–561 (1997)

IJP B
- an international journal

Multiphoton excitation dynamics of polyatomic molecules in picosecond scale under laser pulses of nanosecond duration

S S Mitra* and S S Bhattacharyya

Department of Materials Science (Atomic and Molecular Physics Section),
Indian Association for the Cultivation of Science, Jadavpur, Calcutta-700 032 India

Received 13 November 1996, accepted 1 July 1997

Abstract : We report a numerical study of the excitation dynamics of an anharmonic four level system by a shaped laser pulse in the pico-second scale, using equations of motion for the density matrix of the four discrete levels coupled by the laser field. Both irreversible loss from the topmost level and dephasing due to intramolecular interactions have been included. Parameters of SF_6 have been used for the modeling. The nature of population histories of the four vibrational levels and the histories of leakages to the quasicontinuum (QC) due to laser pulses of slowly or rapidly varying intensity profiles with frequencies tuned to one, two and three photon resonances have been studied in detail. The influence of transverse relaxation introducing incoherence into the excitation process on the population histories of the four vibrational levels and on the leakage to QC has also been investigated. The results show that the excitation dynamics in the picosecond scale are significantly different for the laser frequencies tuned to one, two and three photon resonances. Rapidly increasing intensity profile of the laser pulse and high transverse relaxations and leakages also alter the excitation histories significantly.

Keywords : Multiphoton absorption, density matrix, Rabi oscillation

PACS No. : 33.80.Wz

1. Introduction

The excitation dynamics of polyatomic molecules under strong laser pulse of various shapes and durations have been studied experimentally by many groups in the last two decades using more and more sophisticated techniques [1–7] and in some cases like CF_3I, information is now available about the population histories at different regions of the vibrational ladder with high temporal resolutions [7]. Theoretical works, until recently, have been confined mostly to studying the response of a ladder of multilevel system to square laser pulses [8–10]. Usually multistate Schrödinger equations are solved to obtain

Present Address Department of Physics, Jogamaya Devi College, 92 S P Mukherjee Road, Calcutta-700 026, India

descriptions of coherent excitations that preserve the phase relationships amongst the probability amplitudes leading to such effects as population (Rabi) oscillations and population trapping. Even within this framework variation of intensity and frequency of the laser pulse and structure of the ladder (anharmonicity, linewidth *etc*) produces many interesting changes in the population histories of the levels. Responses of such systems to square laser pulses of different intensities and frequencies have been described by Shore *et al* [11] for both leaky and lossless ladder of states. It has been shown that if the leakage rate from the top (N-th) level is much larger than the corresponding Rabi frequency then the last transition is ineffective and the system behaves like a ladder with (N-1) levels. Other processes that suppress the phase relationship (coherence) like various relaxations in the lower discrete region of the laser absorbing mode of a polyatomic molecule should produce equally interesting change in the population histories of different levels of the system. Such damping terms are generally introduced empirically in a Bloch equation – density matrix description of the excitation process which, unlike the time dependent Schrödinger equation, deals directly with the probabilities [12].

Studies of multiphoton excitation and dissociation of polyatomic molecules under square laser pulse of nanosecond duration had been carried out by several authors in the early eighties using models of multilevel systems with transverse relaxations and loss to QC within the framework of Bloch equations of the density matrix of the system [13–18]. These studies investigate the time averaged properties of the molecules like frequency response and fluence and temperature dependence of multiphoton absorption (MPA) and dissociation (MPD), energy distribution of population in the QC, the nature of discrete level bottleneck, collisional hole filling effect, *etc*, under square laser pulses. However, the influence of the intensity change of shaped laser pulses on the population histories in the different levels of the discrete region were not studied in detail although the interest in using the shape of the pulse to populate a given vibrational state preferentially, 'beating intramolecular vibrational relaxation', dates back to the early days of infrared multiphoton dissociation studies [2,5,10]. Attempts to do this by shortening the pulse length and increasing the intensity failed initially because of complete loss of selectivity due to power broadening. But the scenario has changed completely over the last few years with the advent of picosecond and femtosecond laser pulses and development of several techniques for selective excitation of molecules using ultrashort pulses [19]. Several studies have indicated that the goal of selective excitation can be achieved by designing pulses of modulated frequency [20] or by properly chosen multifrequency phase locked pulses [21] instead of a single monochromatic pulse. In this connection mention may be made of Rabitz and coworkers [22] who instead of arbitrarily choosing a pulse shape, proceeded from first principle and used the Optimal Control Theory (OCT) to optimize systematically the pulse shape for achieving selective excitation to specific target states. Direct experimental confirmation of these pulse shapes recommended by OCT is also now being looked for. In the meantime, it seems to be necessary to study the special features of the response of the multilevel systems to variously shaped laser pulses of short duration.

In a recent paper [23], a simple molecular model has been investigated by the present authors using laser pulses of various shapes including Gaussian and multimode pulses. We compared the results with those obtained using constant intensity laser of same fluence (5 J/cm^2), frequency and duration. This model including both the discrete region and the QC concentrated primarily on how the shape of the laser pulse affects the leakages to QC, the temporal and energy distribution of populations at different regions of QC and the total absorption. It was shown that inclusion of phase relaxation enhances excitation considerably and the absorption due to shaped laser pulse was found to be greater than the corresponding constant intensity pulse of same frequency, fluence and duration with the frequency slightly on the red of the one photon resonant frequency. The effect was found to be less in the frequency region where the bottleneck is very low *e.g.*, at the three photon resonance frequency or very high *e.g.* when the frequency is blue shifted from the fundamental. The excitation histories in the discrete region, however, were not reported in detail. In the present paper we investigate these excitation histories in the discrete region for two different Gaussian pulse shapes of 15 ns duration with one (F2) having fluence 8 times that of the other (F1).

The paper is organised in the following manner : in Section 2 we discuss the mathematical methods and computational techniques used. We have omitted some of the equations which can be found in reference [23]. In Section 3 we present the results and conclude in Section 4.

2. Mathematical formulation

The multilevel optical Bloch equations describing the time evolution of population in the discrete region can be written in the form

$$\frac{d\rho_{vv}}{dt} = \frac{i}{\hbar}[\rho, H]_{vv} - \Gamma_{vk}\rho_{ks}, \qquad v, k, s = 0, 1, 2, 3 \tag{2.1}$$

and $\Gamma_{vv} = 0$ for $v \neq 3$. Here Γ_{vk}'s are the intramolecular relaxation terms when $v \neq k$ caused by the couplings with a heat bath provided by other modes and Γ_{33} is the rate of leakage that occurs from the top of the ladder to the QC. This rate is proportional to the intensity and hence is time dependent. The matrix elements of H for field of amplitude $E(t)$ and frequency ω_L are given by

$$\begin{aligned} H_{vv} &= \varepsilon_v = v\omega_0 + X_{33}v(v-1); \\ H_{v\,v-1} &= H_{v-1\,v} = -\mu_{v,v-1}E(t)\cos\omega_L t \text{ and} \\ \mu_v &= v^{1/2}\mu_{01}; \end{aligned} \tag{2.2}$$

where X_{33} is the anharmonicity of the laser absorbing (ν_3) mode and μ_{01} is the dipole matrix element for $0 \rightarrow 1$ transition. We use $X_{33} = -1.7426$ cm^{-1} and $\mu_{01} = 0.437$ D, the parameters used in our earlier works for the ν_3 mode of SF_6 [25,27]. Using a transformation of the form

$$\rho_{ij} = \hat{\rho}_{ij}\exp(iv\omega_L t) \text{ with } v = j - i \tag{2.3}$$

and making the rotating wave approximation we get a set of 16 equations for the density matrix elements. The off diagonal relaxation terms (T_2-relaxation) are taken as

$$\Gamma_{vs} = \left(g_v + g_s\right) H_{anh}^2; \quad v \neq s \tag{2.4}$$

as assumed in [13, 14 and 16]. Here g_v and g_s are the density of states at the initial and final energy levels and H_{anh} is generally treated as an adjustable parameter estimating the line width in the discrete region. The QC is assumed to begin where $gH_{anh} > 1$ [13–18]. It can be shown that the loss term from the uppermost state ($v = 3$) causes an extra off diagonal relaxation term $(1/2)\Gamma_{33}$ in the Bloch equations connecting all states to this state ($v = 3$) from which loss occurs [24].

As shown earlier, the 16 coupled equations can be transformed into 15 equations with real coefficients using the following transformations [24, 26]

$$\left.\begin{aligned} u_{vs} &= \hat{\rho}_{vs} + \hat{\rho}_{sv} \\ w_{vs} &= \hat{\rho}_{vs} - \hat{\rho}_{sv} \end{aligned}\right\} \quad \text{for } v \neq s \tag{2.5}$$

and

$$w_{vs} = \rho_{vv} - \rho_{ss} \tag{2.6}$$

with $v, s = 0, 1, 2, 3$. The remaining equation can be formulated as expressing the change in total population in the four levels w_4 due to leakage from the topmost level

$$w_4 = \rho_{00} + \rho_{11} + \rho_{22} + \rho_{33} \tag{2.7}$$

The transformed equations with real coefficients and the method of solution are given in the appendices in reference [23]. This set of equations for these transformed variables written in the matrix form

$$\boldsymbol{W} = \boldsymbol{M}\,\boldsymbol{W} \tag{2.8}$$

can be solved in time steps over which $\boldsymbol{M}$ is almost constant. In our calculations the total time over which the equations of motion are integrated is 15 ns. Though rather coarse grid size of 0.33 or 0.167 ns gives a fairly satisfactory convergence for the populations at different discrete vibrational levels and the time dependent loss rates averaged over a few Rabi periods and the total loss to QC, the Rabi oscillation of the populations themselves must be described only with a time step several times less than the Rabi time period. For the shaped laser pulses used in our calculations the Rabi period varies between 35 and 200 picosecond. We use a time step of 10 ps for all calculations presented here. The value of the loss term is chosen to match the cross section for $3\nu_3 \rightarrow 4\nu_3$ transition obtained for the frequency 948 cm^{-1} at the same intensity in [25]. This gives $\Gamma_{33} = 0.01126$ cm^{-1} at 10^8 W/cm^2. The values of different relaxation terms calculated with $H_{anh} = 0.01$ cm^{-1} (as assumed by many authors for SF_6 [13,17]) are as follows: $\Gamma_{01} = 0$; $\Gamma_{02} = 0.001$ cm^{-1}, $\Gamma_{03} = 0.00222$ cm^{-1}, $\Gamma_{12} = 0.0015$ cm^{-1}; $\Gamma_{13} = 0.00262$ cm^{-1} and $\Gamma_{23} = 0.00312$ cm^{-1}. Thus the leakage induced coherence-loss term $(1/2)\Gamma_{33}$ connecting $v = 0, 1, 2$ with $v = 3$ is either comparable or greater in magnitude to the T_2^{-1} dephasing terms. It has been shown in

reference [23] that the phase relaxations enhance the overall excitation to the higher vibrational states significantly [3].

3. Results and discussion

In Figure 1, the intensity profile for the two different pulse shapes F1 and F2 used in this study, are shown. The inset shows the time dependence of fluence of these two pulses

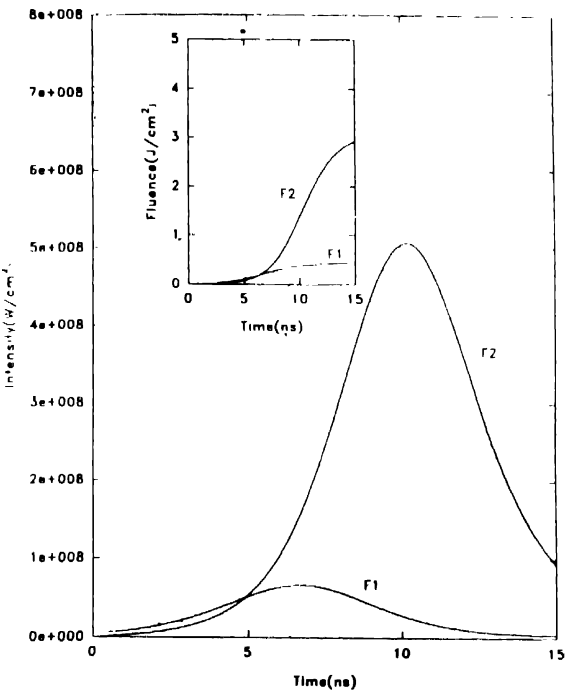

Figure 1. Intensity profiles of the laser pulses (F1 and F2) of duration 15 ns
Inset Fluence *versus* time plot for the two shaped laser pulses (F1 and F2)

(The functional forms and values of the parameters used to generate the pulse shapes are given in Appendix–I). The two pulses are 15 nano second long having a single peak at around 7 and 10 ns respectively. Although their shapes are similar, the peak intensity of F2 is nearly 8 times that of F1. The time step of 10 ps used for calculation is smaller than the minimum Rabi time period at the peak intensity. Integrated quantities like total loss, average loss rates and average populations of different states have been found to converge even for a crude step size of 0.33 nanosecond.

In the next three sets of Figures (Figures 2–4), the population histories of the 4 discrete levels are shown from the beginning of the pulse upto 3 ns using three different laser frequencies. In all these cases, the pulse shape was F1. The frequencies used are

948 cm^{-1}, 946.2574 cm^{-1} and 944.5148 cm^{-1} which correspond to one $(\varepsilon_1 - \varepsilon_0)$, two $\left((\varepsilon_2 - \varepsilon_0)/2\right)$ and three photon $\left(\varepsilon_3 - \varepsilon_0)/3\right)$ resonance frequencies between the state $v = 0$ and $v = 1$, 2 and 3 respectively. ε_v is the energy of the vibrational level v. The intensity of the pulse F1 is quite low upto 3 ns and these plots show the low intensity response of the

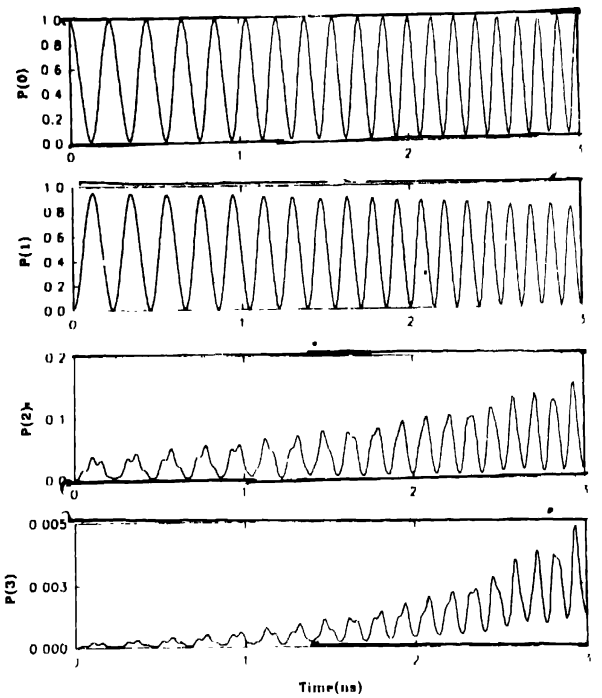

Figure 2. The population histories of the four vibrational levels $v = 0 - 3$ between 0 and 3 nanosecond for the laser pulse shape F1 and $\omega_L = 948$ cm^{-1}, calculated using 10 ps time steps

system when both the dynamic Stark shifts and power broadening of different states are small. When ω_L is 948 cm^{-1} (Figure 2) the system initially behaves like an isolated two level system with all the population remaining confined to the first two levels due to resonance. The probabilities of occupation of the levels $v = 0$ and $v = 1$ ($P(0)$ and $P(1)$ respectively) oscillate between the values 0 and 1 in opposite phase with time period of 0.2 ns approximately as expected in a two level system with zero detuning. Populations in $v = 2$ and 3 are insignificant but as the intensity of the laser pulse increases with time a larger fraction of population is pushed up from $v = 0$ to $v = 2$ and 3 because of power broadening and shift of the dressed states. Thus the maximum population in $v = 1$ decreases slowly with increasing time. The populations of all the excited states oscillate nearly in phase initially but with increasing intensity of the pulse the flopping period decreases and

they go out of phase. Loss to the quasicontinuum from $v = 3$ is insignificant during this interval (0 – 3 ns).

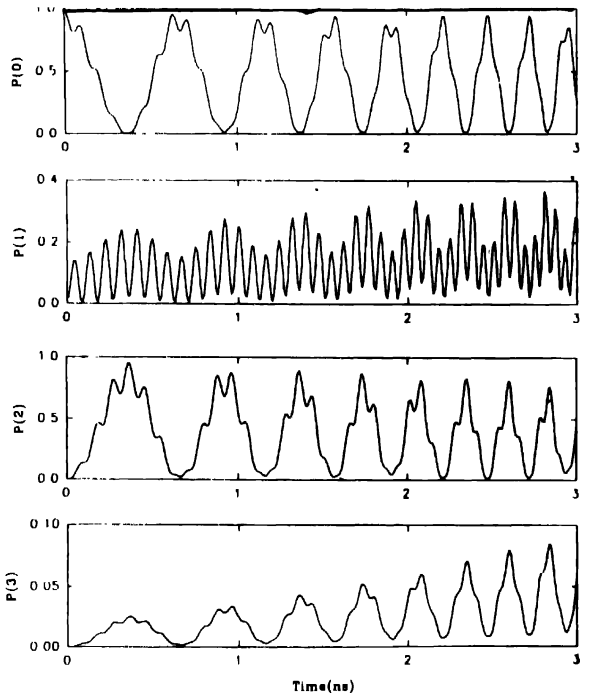

Figure 3. Same as in Figure 2 but for $\omega_L = 946\ 2574\ \text{cm}^{-1}$

In Figure 3, the population histories of the four levels for the same laser pulse and in the same time interval are shown when the laser frequency is 946.2574 cm^{-1} *i.e.*, when $v = 0$ and $v = 2$ are in two photon resonance. Here, as expected, the population is initially confined to $v = 0$ and $v = 2$ with period of oscillation 0.6 ns. The oscillation of $P(0)$ and $P(2)$, however, shows structures since a significant fraction of population oscillates between $v = 0$ and 1 with a different period. The period of oscillation of $P(1)$ is about 0.08 ns with an envelop oscillation of period 0.6 ns superimposed on it. The smaller period for oscillation of $P(1)$ is due to large positive detuning of $v = 1$ with respect to ω_L. The time period for oscillation for two photon excitation from the ground state is nearly three times that for one photon resonant excitation (Figure 2). As the intensity of the laser pulse increases with time, the populations in all the 4 levels oscillate faster and the locally time averaged populations in $v = 1$ and 3 become significant. It should be noted that in the initial period when the loss to QC is almost zero the total probability (population) in the four states is conserved and merely cycles through the states. Probabilities being absolute squares of amplitudes oscillating at combination of frequencies, involve sums and differences of

eigenfrequencies. It has been shown in [11] that for a three state lossless resonant excitation the period of the middle state of the ladder is half of that of the first and the last states. The small positive detuning for $v = 1$ also reduces the time period further. This does not occur for $P(3)$ ($v = 3$ has negative detuning) which oscillates with almost the same time period as $P(0)$ and $P(2)$ *i.e.*, 0.6 ns initially.

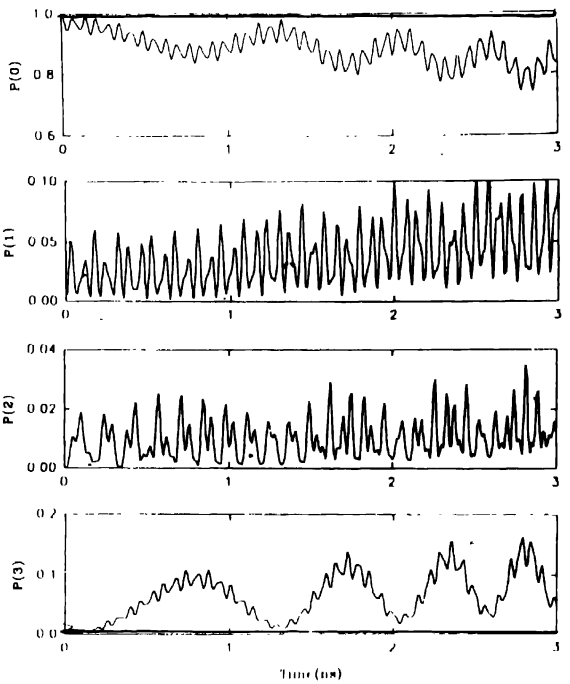

Figure 4. Same as in Figure 2 but for $\omega_L = 944.5148\ \text{cm}^{-1}$

Figure 4 presents the population histories for the 4 levels when the pulse frequency is 944.5148 cm^{-1}. At this frequency three photon resonance strongly couples $v = 0$ and $v = 3$ initially when the intensity of the pulse is low. As seen from the plot the history of excitation presents a completely different picture here. The three photon Rabi period is very large initially *i.e.*, about 1.2 nanosecond but decreases with increasing intensity of the laser pulse. It is well known that [11] n-photon resonance Rabi oscillation is always slow compared to the characteristic single photon response time. The faster oscillation superimposed on it is due to populations flowing in and out of $v = 1$ and 2. The oscillations of $P(1)$ and $P(2)$ are irregular with initial period of about 0.07 ns. The most striking feature is the incomplete modulation of the ground state population even at the beginning of the pulse when resonance is perfect between $v = 0$ and $v = 3$. Unlike one or two photon resonance where the amplitude of oscillation of $P(0)$ is almost 1 initially, here it is never more than 0.3 around the mean value which decreases further with decreasing total

populations due to loss and increasing intensity of the pulse. Although the intensity of the pulse in the beginning is insufficient for appreciable three photon excitation the incomplete

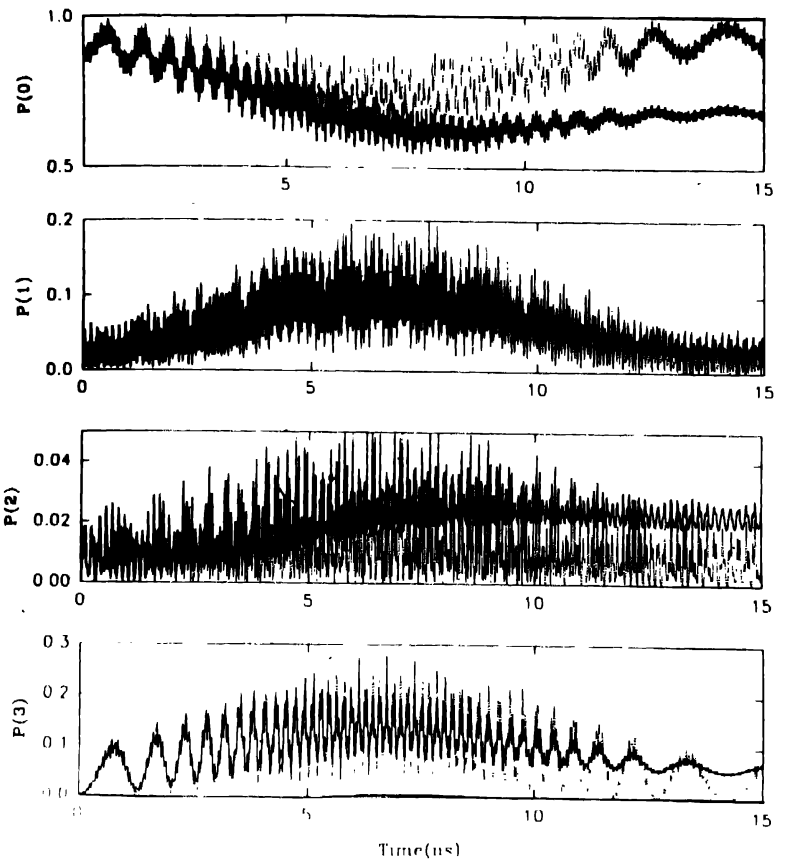

Figure 5. $P(v)$ as functions of time for $v = 0 - 3$ when $\omega_L = 944.5148$ cm^{-1} and pulse shape F1 between 0 and 15 ns. Full lines show the results when loss and relaxations are included and dashed lines show the results when they are not included in the excitation model

modulation will persist throughout the pulse even in the region where the intensity is comparatively high. This is the hallmark of large detuning of the intermediate states. Another interesting point to note is that although the static detunings of $v = 1$ and 2 at this frequency are same (3.4852 cm^{-1}), the average population in $v = 1$ is three times as large as the average $P(2)$ throughout the pulse duration. This indicates the relative inefficiency of two photon excitation compared to one photon excitation at the same intensity. The full line graphs in Figure 5 show the same population histories as shown in Figure 4 for the complete pulse time (15 ns). $P(3)$ is never more than 0.2 inspite of three photon resonance. Apart from the low peak intensity of F1 and large detuning of the intermediate states, loss

from $v = 3$ to the quasicontinuum and relaxations between $v = 2$ and 3 may be responsible for this low value of $P(3)$.

One of the main purposes of this numerical experiment was to study the influence of the transverse relaxations and loss on the population dynamics of the 4-level system driven by a shaped laser pulse. Figure 5 also compares the population histories of the four levels with (case-I) and without (case-III) transverse relaxations and loss for $\omega_L = 944.5148$ cm^{-1} for the pulse shape F1 over the whole pulse length. The full and dotted

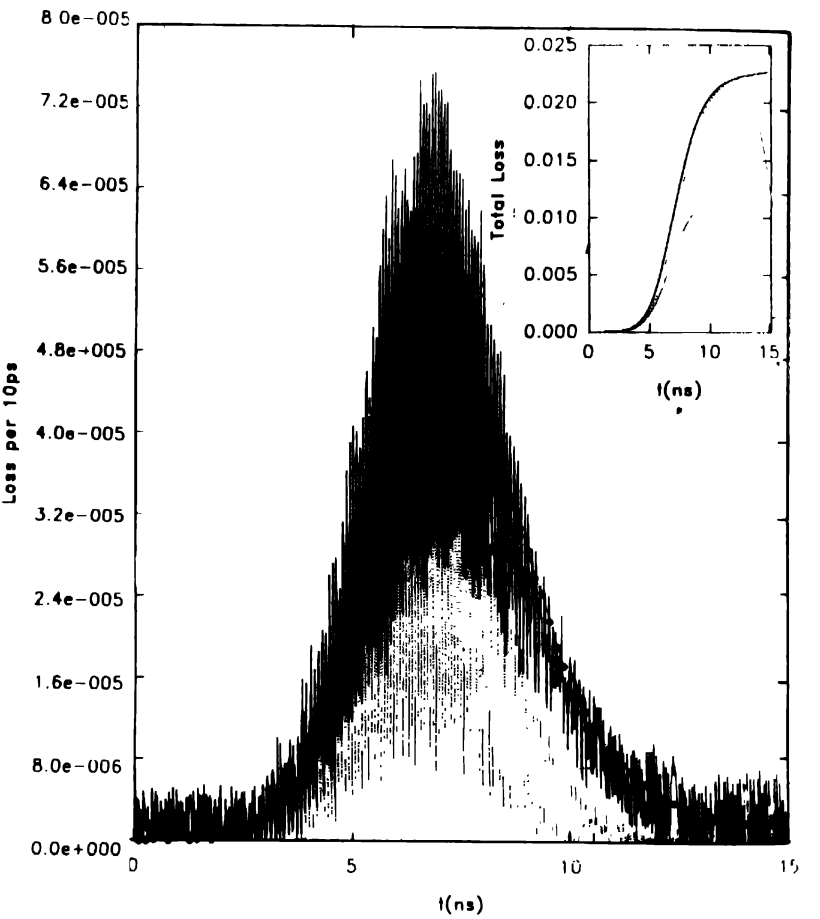

Figure 6. Loss rates (loss per 10 ps) versus pulse time upto 15 ns for the laser pulse F1 of frequency 948 cm^{-1} calculated using 10 ps time steps. The symbols show same loss rates calculated using 0.167 ns time steps. The dashed lines show the results when transverse relaxations are not included.

Inset : Total loss to QC calculated using the same pulse as mentioned above (Figure 6) with 10 ps step size, is shown by full line and with 0.167 ns step size by dashed line. The dashed line below shows the total loss *versus* time when relaxations are not included

lines show population histories for cases I and III respectively. In case III, the excitations of the four anharmonically shifted nondegenerate isolated levels are fully coherent. In case II (not shown in the figure) excitations without loss to QC is studied retaining the transverse relaxations. The population histories of the 4 levels are almost unaffected by loss initially except a noticable decrease of the peaks of the populations of $v = 0$, 2 and 3 levels. P (1) is, however, completely unaffected. This is predictable since loss is proportional to the instantaneous population of the topmost level and most of the leakage occurs from the peaks of P (3). The ground state population, however, gains again at the end of the pulse with decreasing intensity in the cases II and III as there is no leakage to QC. In case III the amplitudes of population oscillations increase significantly for all the four levels bringing back near complete modulations particularly for P (0), P (2) and P (3). The populations now oscillate between 0 and the maximum value in a more regular fashion. While P (2) and P (3) are affected mostly in the lower part reducing the average population in $v = 2$ and 3, the mean value of P (0) is increased mainly at the end of the pulse due to the absence of loss. When the transverse relaxation terms are put equal to zero but loss terms are retained P (0) is increased only around the peaks increasing the mean value. Thus, transverse relaxations primarily reduce the flow back of populations to the ground state by reducing the induced emissions and causes slow accumulation of populations in the excited states increasing the loss.

Figure 6 shows the plot of leakage rates (loss per 10 ps) *versus* time with and without relaxation for pulse of shape F1 with $\omega_L = 948$ cm^{-1}. The plot for the latter is shown by dashed lines. The inset shows the corresponding total loss. The averaged loss rates obtained with a time grid of 10 ps agree well with the rates obtained with a coarse grid of 0.33 ns shown by the dots. The total loss is also unchanged when a coarser grid is used. As shown in the inset, the total loss decreases sharply if transverse relaxations are put off. Since the leakage rates are proportional to P (3), the amplitude and the period of oscillation of it follow the history of P (3). It should be noted that the absence of relaxation not only reduces the leakage rates but also reduces the width of the temporal distribution of the leakage rates. In Figure 7, the same variations are shown for $\omega_L = 946.2574$ cm^{-1}. Here the bottleneck to excitation is lower compared to the previous case due to two photon resonance. Thus the leakage rates are nearly one order of magnitude higher than that obtained with $\omega_L = 948$ cm^{-1}. Unlike the previous case the width of the temporal distribution of the leakage rates is unaffected by relaxations. The dashed curve shows the leakage rates without the transverse relaxations. The minima of the leakage rates are now almost zero and the total loss (shown in the inset) decreases significantly due to the absence of relaxations. It has been observed that relaxations play an even less significant role at $\omega_L = 944.5148$ cm^{-1} where three photon resonance directly couples $v = 0$ and 3. The decrease in total loss due to the absence of relaxations is negligible at this frequency. This

can be inferred from Figure 5 also. Although the amplitude of oscillation of P (3) is larger without relaxations, the average P (3) populations are almost the same except at the end of the pulse.

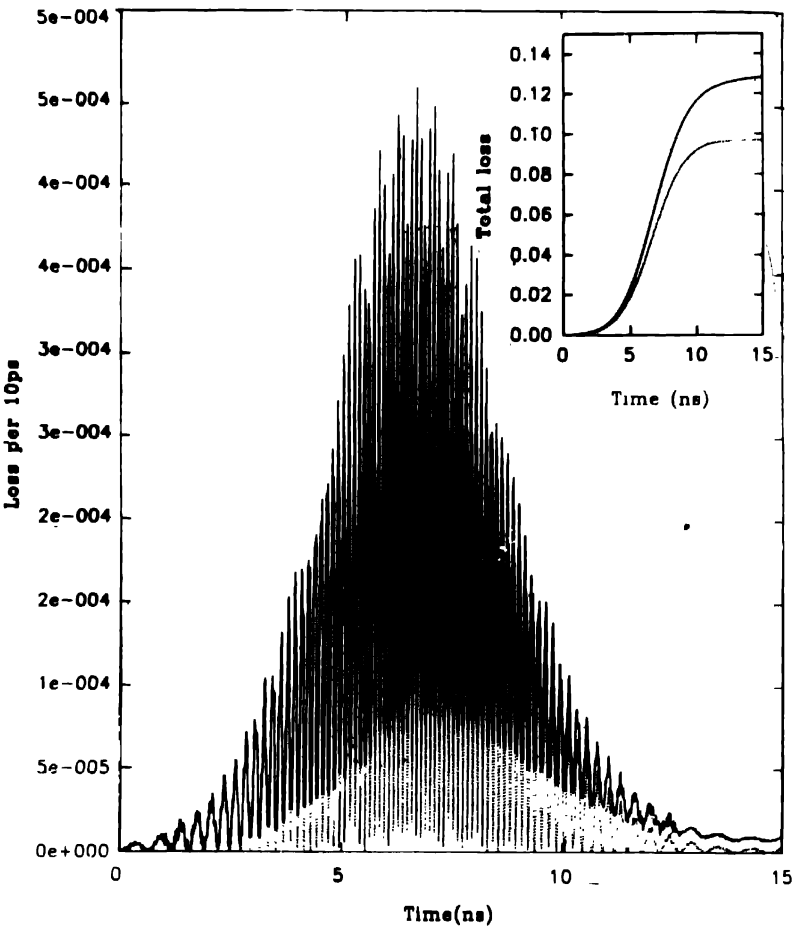

Figure 7. Loss to QC per 10 ps versus time due to laser pulse F_1 of frequency 946.2574 cm^{-1}
Inset : Total loss to QC calculated using the same pulse as mentioned above (Figure 6) with 10 ps step size is shown by full line. The dashed line below shows the total loss *versus* time when relaxations are not included

Figures 8 and 9 show the population histories for the four levels between 7 and 13 ns when pulse shape F2 is used with ω_L = 948 and 946.2574 cm^{-1} respectively. As mentioned earlier, the peak intensity of this pulse is nearly 8 times larger than the peak value of F1 and the total fluence is 7 times that of F1. The initial response is almost the same as in the case of F1 but with rapidly increasing intensity of the pulse, the time period of oscillation

decreases sharply. For ω_L = 948 cm^{-1} the amplitudes of oscillations of P (0) and P (1) decrease and those of P (2) and P (3) increase with time. At around 7.95 ns the oscillation

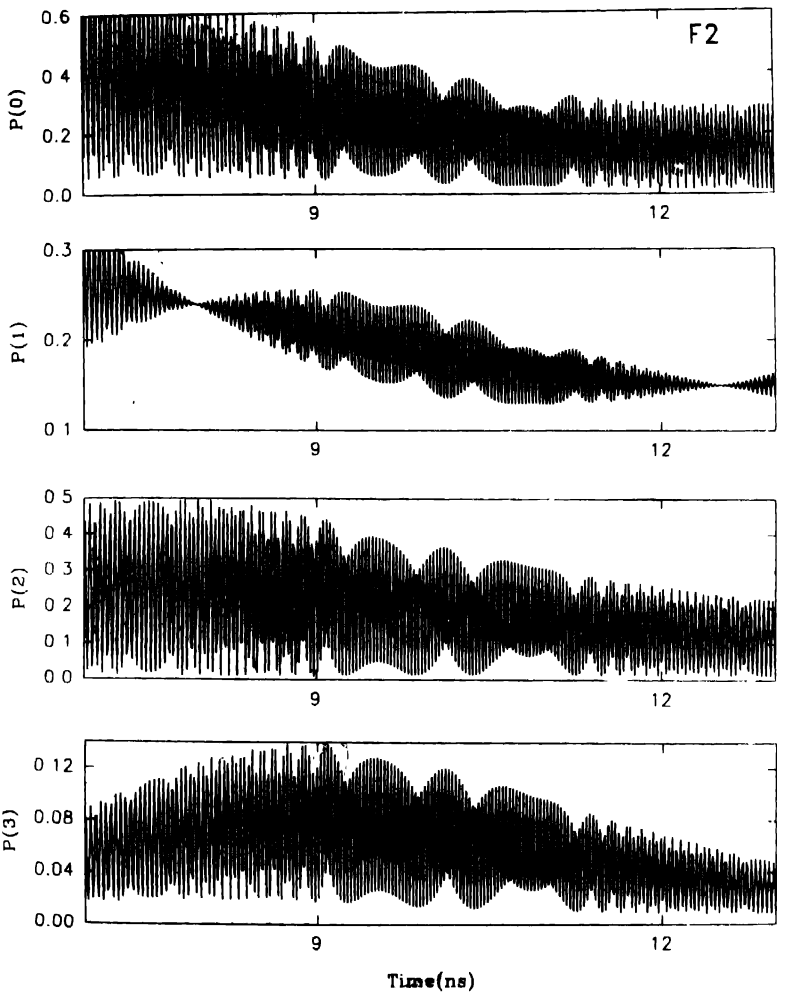

Figure 8. The population histories of the four vibrational levels v = 0 – 3 between 7 and 13 nanosecond for the laser pulse shape F2 and ω_L = 948 cm^{-1} calculated using 10 ps time steps.

of P (1) is completely stopped for about 0.05 ns and then starts again with very low amplitude. It again becomes zero at around 12.5 ns. The amplitude of oscillation of P (2) is, on the other hand, maximum at 7.95 ns. The intensities of the pulse at 7.95 and 12.5 ns are same *i.e.*, 3 × 10^8 W/cm^2. At this intensity, it seems, the Rabi oscillation for v = 1 is critically damped. The position and the nature of this damping are unaffected by the

absence of relaxations and loss. A square pulse of intensity 3×10^8 W/cm^2, however, shows significant excitation to $v = 1$ with normal oscillation of P (1). This type of complete damping of oscillation of population is not observed for other two laser frequencies used.

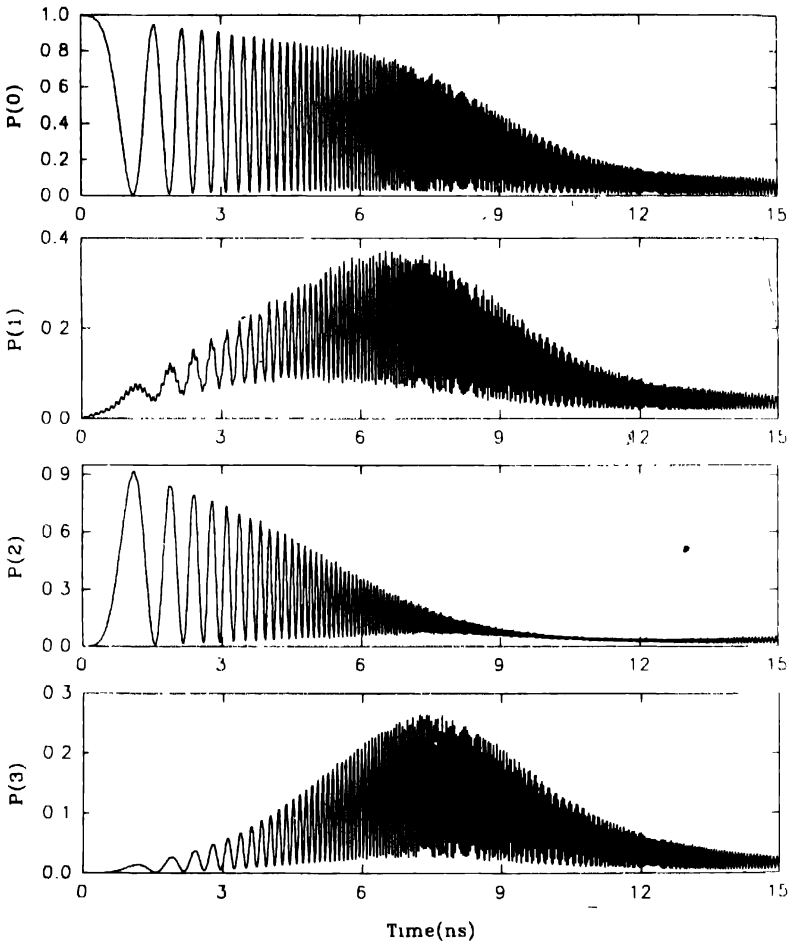

Figure 9. Same as in Figure 8 but for $\omega_L = 946\ 2574$ cm^{-1}

At 946.2574 cm^{-1}, the low intensity response is similar to that obtained with F1 (Figure 3) but with rapidly increasing intensity P (1) and P (3) increase while P (0) and P (2) decrease rapidly. Although the peak intensity of the pulse occurs at around 10 ns, the average populations in all the 4 levels decrease beyond 7 ns due to significant loss of the population to QC. The oscillation of P (2) around the peak intensity (10 ns) is highly damped but unlike the previous case its amplitude is never zero.

Figure 10 shows the population histories upto 10 ns for the three photon resonance frequency 944.5148 cm^{-1} with pulse shape F2. The full lines show the histories when transverse relaxations (TR) Γ_{ij} are not included in the descriptions and the dashed lines show the same when both TR and loss to the QC are excluded. The absence of loss not only

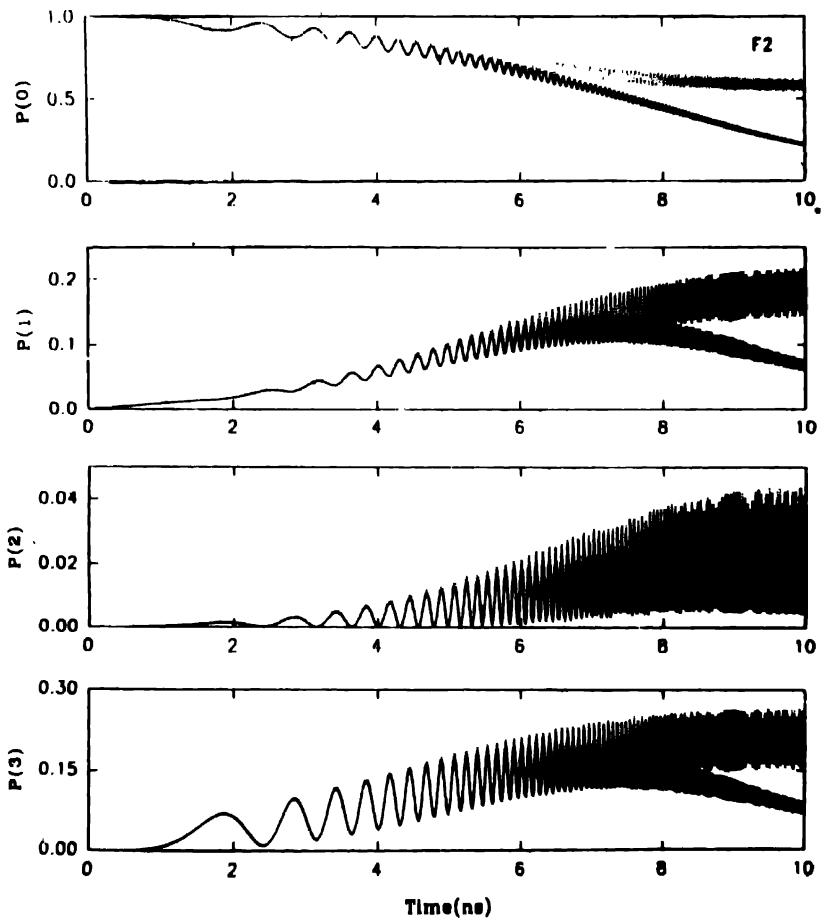

Figure 10. $P(v)$ as functions of time for $v = 0 - 3$ when $\omega_L = 944\ 5148\ cm^{-1}$ and pulse shape F2 within 0 and 10 ns. Full lines show the results when loss and relaxations are included and dashed lines show the results when they are absent

increases average populations of all the four levels but also increases the amplitudes of oscillations of all the four levels since irreversible loss from the topmost level introduces an incoherence into the system. If TR are included in the description, amplitudes of oscillations of populations in all the four levels show further decrease and the average value

of P (2) increases by 50% around the peak and 100% at 10 ns. The total loss to QC is also unaffected here with or without TR. If we compare the population histories for pulse shapes F1 and F2 at the same laser frequency (Figures 5 and 10), we can see that all the secondary structures in oscillations of populations due to the slowly varying low intensity pulse shape F1 have disappeared in the case of F2. The oscillations are quite regular now with amplitudes of oscillations less than those obtained with F1. Thus sharply varying intensity of the laser pulse modifies the population histories significantly suppressing irregularities in the population oscillations.

4. Conclusions

(1) Even at very low intensity of the laser pulse excitation histories of the four discrete anharmonically shifted levels are complex and deviate significantly from the response of an isolated two level system particularly for two and three photon resonance frequencies.

(2) Both long and short time periodicities are strongly affected by the intensity profile of the laser pulse through Stark shift and power broadening. A laser pulse with rapidly varying intensity profile, however, forces the excited state populations to oscillate in phase suppressing all irregular structures.

(3) Presence of large negative intermediate state detuning causes incomplete modulation of ground and excited state populations even at multiphoton resonance frequency

(4) Transverse relaxation and loss to QC introduce incoherence in the excitation process reducing the amplitudes of oscillations of populations in the ground and excited states. The absence of relaxations not only reduces the total loss to QC but also the width of the temporal distribution of the loss rates.

(5) With rapidly varying pulse shapes it is possible at certain frequencies to completely suppress population oscillations in one of the excited states temporarily.

References

[1] Chemistry by IR laser (Special Issue) *Spectrochim. Acta.* **43** No. 2 (1987)

[2] V N Bagratashvilli, V S Letokhov, A A Makarov and E A Ryabov *Laser. Chem.* **1** 211 (1983), **4** 1 (1983); **4** 311 (1984)

[3] D W Lupo and M Quack *Chem. Rev.* **87** 181 (1987)

[4] A M Weiner, D E Leaird, G P Wiederrecht and K A Nelson in *Coherence Phenomena in Atoms and Molecules in Laser Field* eds. A D Bandrauk and S C Wallace (New York · Plenum Press) p 277 (1992)

[5] G Hancock and A J McRobert *Chem. Phys. Lett* **101** 312 (1983)

[6] J L Lyman, G P Quigley and O P Judd in *Multiple Photon Excitation and Dissociation of Polyatomic Molecules* ed. C D Cantrell (Berlin · Springer) p 9 (1986)

[7] M Quack, R Schwartz and G Seyfung *J. Chem. Phys.* **96** 8727 (1992)

[8] C D Cantrell, V S Letokhov and A A Makarov in *Topics in Current Physics : Coherent Nonlinear Optics* eds. M S Feld and V S Letokhov (Berlin : Springer) p 165 (1981)

[9] D P Hodgkinson, A J Taylor, D W Wright and A G Robiette *J. Phys.* **B14** 1803 (1981)

[10] D M Larsen and N Bloembergen *Opt Commun.* **17** 254 (1976)

[11] B W Shore in *The Theory of Coherent Atomic Excitation* **Vol 2** (New York Wiley Interscience) p 949 (1990)

[12] J Stone in *Lasers, Molecules and Methods . Advances in Chemical Physics* **Vol LXXIII** eds J O Hirschfelder, R E Wyatt and R D Coalson (1989)

[13] M F Goodman, J Stone and E Thiele in *Multiple Photon Excitation and Dissociation of Polyatomic Molecules* ed C D Cantrell (Berlin . Springer) p 159 (1986)

[14] A Horsley, J Stone, M F Goodman and D A Dows *Chem Phys Lett* **66** 461 (1979)

[15] J Stone *Phys Rev* **A26** 1157 (1982), **30** 2517 (1984)

[16] M F Goodman, J Stone and D A Dows *J Chem Phys.* **65** 5052 5062 (1976)

[17] H Johansen and R Muller *Spectrochim Acta* **43A** (1987)

[18] E Borsella, R Fantoni, A Ferretti, A Giardini-Guidoni, M Dilonardo and J Reuss *Chem. Phys* **94** 309 (1985)

[19] M Quack and J Stohner *J. Phys Chem.* **97** 12547 (1993)

[20] S Chelkowski and A D Bañdrauk in *Coherence Phenomena in Atoms and Molecules in Laser fields* eds A D Bandrauk and S C Wallace (New York · Plenum) p 333 (1992)

[21] P Brumer and M Shapiro *Annu Rev Phys Chem* **43** 257 (1992)

[22] H Rabitz in *Coherence Phenomena in Atoms and Molecules in Laser fields* eds A D Bandrauk and S C Wallace (New York Plenum) p 315 (1992)

[23] S S Mitra and S S Bhattacharyya *J Phys* **B29** 5735 (1996)

[24] I Schek and J Jortner *Theor Chem Acta* **69** 323 (1986)

[25] S S Mitra and S S Bhattacharyya *J Phys* **B23** 1453 (1990), **25** 2535 (1992); **27** 6761 (1994)

[26] R G Brewer and E L Hahn *Phys. Rev* **A11** 1641 (1975)

[27] M M Samanta, S S Bhattacharyya and S S Mitra *Indian. J Phys* **61B** 496 (1987)

Appendix - I

The general expression for the intensity profiles of the laser pulses used in this study is

$$I_j = A\left(t/(t+Q)\right)\left[B\ \mathrm{Sech}\left[\left((t-C)/D\right)^2\right]\right], \qquad \text{(II.1)}$$

where I_j is the intensity for the pulse shape F_j (F_1 or F_2), t is the time measured in nanosecond and A, Q, B, C and D are adjustable parameters. Their values are given in Table I below.

Table 1. Parameters used to generate different pulse shapes.

Pulse	Q	A [W/cm^2]	B	C [ns]	D [ns]
F_1	0	44.2×10^7	0.15	20/3	10/3
F_2	20/3	8.645×10^8	0.95	10	3